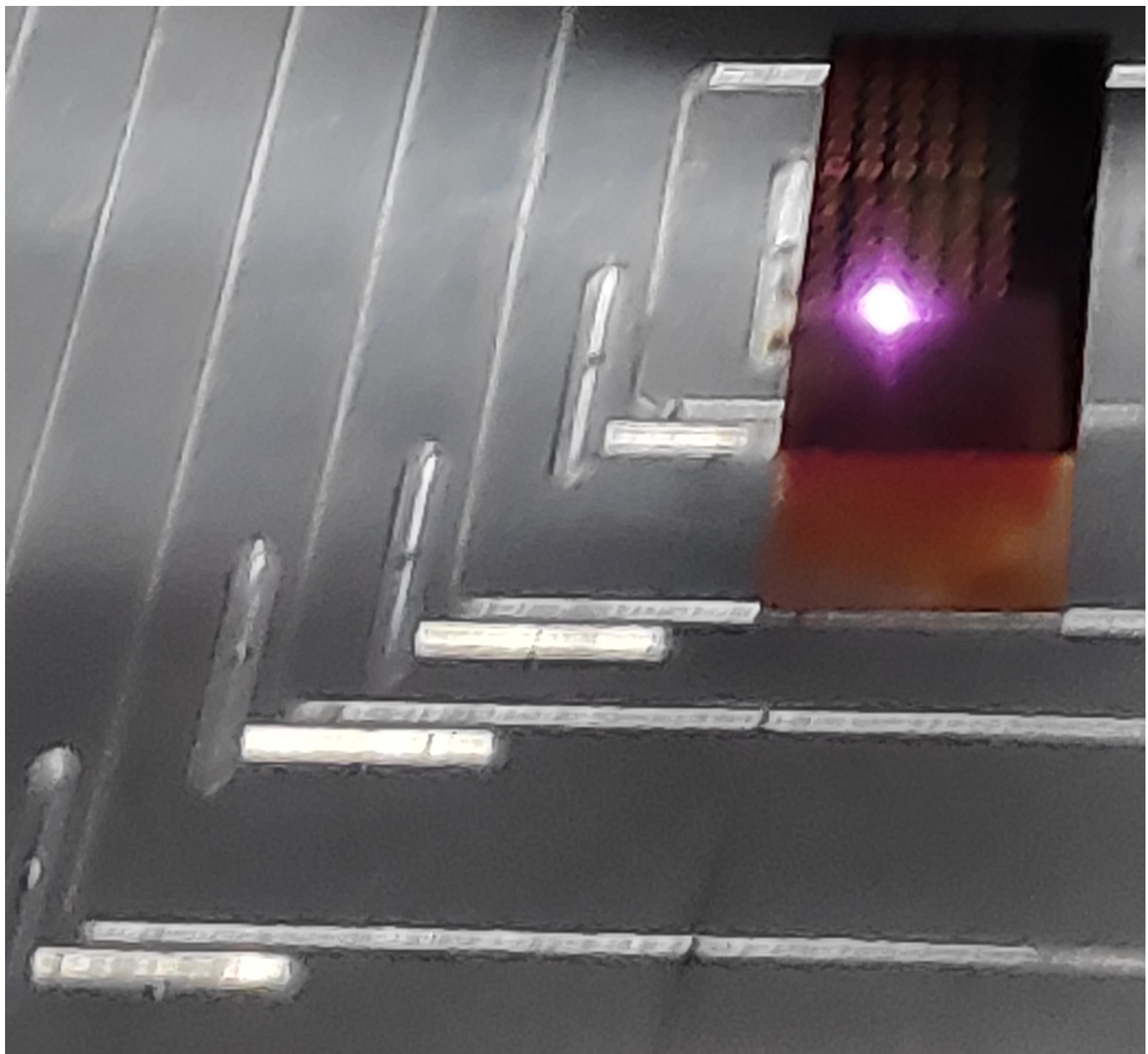


Internship report: Photonic structure fabrication by use of ultrashort laser pulses



Intern: Iheb DAALOUL

internship supervisor: Nicolas SANNER

Duration: from 09/03/2020 to 09/07/2020

Location: LP3 Laboratory (Marseille)

Contents:

Introduction

I/ Passive optical metasurfaces and photonic crystals

- 1.1/ What are optical metasurfaces?
- 1.2/ How optical metasurfaces work
- 1.3/ Photonic crystals
- 1.4/ Example of a photonic crystal structure and comparison with laser technique capability

II/ Nanofabrication techniques

- 2.1/ Direct write lithography
- 2.2/ Pattern transfer lithography techniques
- 2.3/ Other techniques for metasurfaces fabrication

III/ Laser techniques

- 3.1/ Physics of ultrafast laser pulses interacting with dielectrics
- 3.2/ Gaussian beams
- 3.3/ Temporal shaping
- 3.4/ Spatial beam shaping
- 3.5/ Combination of laser irradiation and chemical etching
- 3.6/ Discussion: comparison of experimental techniques
- 3.7/ Overview

IV/ Analysis techniques of laser nanofabricated structures

- 4.1/ Scanning electron microscopy
- 4.2/ Atomic force microscopy
- 4.3/ Light microscopy

Introduction

This document is an internship report made for the end of the second year of the nanosciences-NDQ master at Aix-Marseille university. The internship was done in the LP3 laboratory, which is located in Marseille. This laboratory works on ultrashort laser matter interactions. The researchers try to understand the physical processes at play in these interactions. They develop new analysis techniques and materials. They also use that knowledge to develop new manufacturing techniques. This internship is linked to that last interest of the LP3 laboratory. As the ablation of dielectric materials with ultrashort lasers has progressed through the years, and has become more and more precise, it is now possible to access the sub-micron scale. With this in mind, we wonder if it is now possible to make sub-micron photonic components. The optical components we are interested in are dielectric metasurfaces and dielectric photonic crystals. The subject of this internship is therefore the exploration of this question. At first we intended to make some of these components but that was not possible due to the COVID-19 pandemic. Therefore, in this text we will only look at the scientific literature in order to answer the question stated previously. In this text we start by defining passive metasurfaces and photonic crystals. We then look at the many nanofabrication techniques that have been used to make similar structures. Following that, we focus on direct writing ultrafast-laser techniques. And finally we rapidly look at the main analysis techniques that are used to characterize nanostructures.

I/ Passive optical Metasurfaces and photonic crystals

In this part of the text we give a definition of passive optical metasurface. We will talk about the different kind of metasurfaces. We then focus on all dielectric metasurfaces and finally, we give examples of projects made with all dielectric metasurfaces.

1.1/ What are optical metasurfaces?

Optical metasurfaces are a suborder of flat optics components. They are a promising technology that could replace traditional 3D, ground, surface lenses and Fresnel lenses. Concave/convex 3D lenses are the oldest type of lenses we know. Their manufacturing processes are well mastered, but it still takes a lot of grinding time to make these lenses [1]. Another problem is that these optical components are bulky. Indeed, a high-end lens system can be made of 20 lenses, spanning 30 cm in length, and having a mass of 4 kg. This problem is solved with Fresnel lenses which are flat, compact and cheap to manufacture; using rapid printing methods that do not require a long polishing time. A problem however, is that these lenses are only efficient at low numerical aperture.

Optical metasurfaces are a superior technology that can overcome the problems of traditional optical components. Metasurfaces can be used to make a lot of optical components such as high efficiency ultrathin lenses [2], broadband reflectors [3], multi-color holograms [1], polarizers and much more [4]. Optical metasurfaces can allow for a high diversity of components because they are made of subwavelength geometrical structures that allow for the control of amplitude, phase, and frequency of incident electromagnetic waves. All these properties can be tuned solely by changing the shape of the geometric pattern at the frontier of air and the substrate of the metasurface. Furthermore, it is possible to control the optical properties with an external signal. That can be done with a voltage, by doping, or by using phase change materials. This type of optical metasurface is called active metasurface and will not be explored in this text. We will only focus on passive metasurfaces.

1.2/ How optical metasurfaces work

Optical metasurfaces are made of a structure of nanoresonator that scatter light and act as wavelets sources (as known to the traditional Huygens' construction)[5]. Depending on how the nanoresonators are placed we can use them to construct an arbitrary wavefront.

Figure 1.1 shows this. It demonstrates how a metasurface can be used to modify the refraction on a boundary between two materials (air/fused silica, for example). Indeed, normally, when we have a normal plane wave at a flat interface, it just passes through while keeping the same angle. However, when we structure the surface, we can modify the wavelets making the exiting wavefront. This results in the exiting plane wave being refracted at the interface, despite having a normal incidence. The angle of refraction can be changed at will by modifying the geometry of the metasurface.

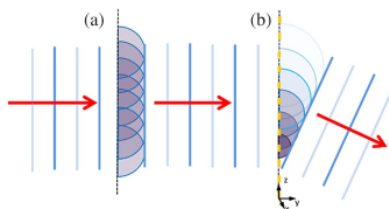


Figure 1.1: Huygens' construction for a metasurface diffracted plane wave; on the left we have the wave propagating through a flat surface; on the right the wave propagates through a nanostructures surface, resulting in a refraction effect; source: [5]

When the nanostructure of the metasurface is made of noble metals (Au, Ag, Al), then the scattering of light happens because of a phenomenon called resonant scattering [5]. This happens

when an incident wave of frequency f , makes the free electrons at the surface of the metal, oscillate. They oscillate with the same frequency f but with a phase delay (ϕ) which can range from 0 to π . If $f \rightarrow 0$ then $\phi \rightarrow 0$, if $f \rightarrow \infty$ then $\phi \rightarrow \pi$. When electrons are oscillated, they emit electromagnetic waves, which are scattered (and in this case phase retarded, compared to the incident wave). Therefore these little metal structures, that compose the metasurface, act as radiating antennae. We can use these subwavelength sources of electromagnetic radiation as wavelet sources and use them to shape a larger wavefront. Their wavefront can have an arbitrary shape that is only dictated by the metal resonators geometry.

Nanoantennae scattering can be done more efficiently if all dielectric nanostructures are used. These subwavelength nanostructures have a high index of refraction contrast and have higher width to depth aspect ratio (>4). The individual nanostructures are 100 to 200 nm in size when dealing with visible light [5]. The structures are dielectric resonators that can scatter light using the electric and magnetic fields of an incoming electromagnetic wave. For metal resonators, only the electric field is used. Once the dielectric resonators are activated by an incident wave, they act as wavelet generators, and can be used to shape the exiting waves' wavefront. Working wavelength can be tuned by changing the geometry and size.

The table in figure 1.2 summarizes the passive types of optical metasurfaces that can be obtained as a function of the physical phenomenon used, the composition, and the size.

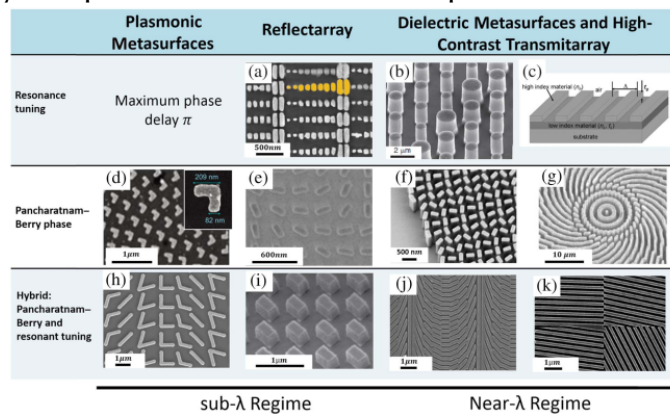


Figure 1.2: The different types of metasurfaces; source: [5]

1.3/ Photonic crystals

Photonic crystals are periodic structures in transparent materials (a matrix of holes for example). The crystals have a spatial period on the order of the wavelength of light[6]. These structures can be three dimensional or 2 dimensional. However 2D photonic crystals are more often used because they are easier to make.

Schematics of 2D and 3D photonic crystal structures are shown in figure 1.3. These periodic structures create an optical band structure in the material. This is similar to the electronic band structures that are seen in semiconductors and that are due to the periodic arrangement of atoms of the lattice. Similarly to the electronic bandgap, which forbids certain energy levels for electrons, we have an optical bandgap in photonic crystals. This bandgap forbids certain light frequencies from propagating through the crystal. When defaults are present in a semiconductor, this creates energy levels in the bandgap. This effect can be replicated in photonic crystals. We can implement defaults in the regular structure of a photonic crystal in order to allow for the propagation of a single wavelength. This allows for the creation of waveguides. These photonic crystals can be used for multiple uses. They can be used to make micro-optical circuits, light filters, sensors, polarizing beam splitters and much more.

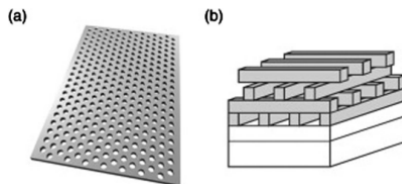


Figure 1.3: Schematic of photonic crystals; (a)2D photonic crystal structure; (b)3D photonic crystal structure; source: [6]

1.4/ Example of a photonic crystal structure and comparison with laser technique capability

If we want an example of a 2D photonic crystal structure, we can look at reference [6]. In that article, we have the example of a structure made of periodic air holes in a Si slab. In this structure is implemented a line defect (a line area without air holes) that serves as a waveguide that propagates light on the thin Si slab. This structure also contains a point defect (removal of one or more air holes). This defect is coupled to the waveguide and can be used to extract or add light into the waveguide at a very specific wavelength (at $\lambda \sim 1583$ nm), from free space. The holes in this structure have a diameter of around 315 nm. The holes are arranged as a triangular lattice and have a spatial period of $a=420$ nm. This structure and it's transmission spectrum are shown in figure 1.3A. This figure also shows the added and removed spectrum of light through the point defect. We note that the many peaks in the transmission spectrum are caused by Fabry-Perot resonance, caused by the edges of the waveguide.

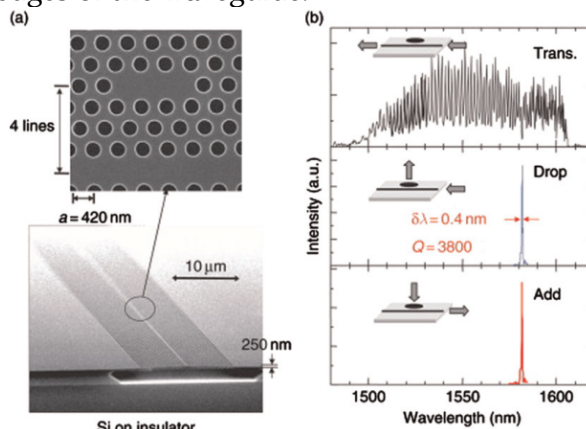


Figure 1.3A: Line defect waveguide structure; (a)Scanning electron microscope image of the nanostructure; (b)Transmission spectrum of the waveguide, & spectrum of the light added or removed from the waveguide through the point defect (which is shown in the zoomed image (a)); source: [6]

Knowing the features sizes of this structure, we can compare it to the channel lattice made by the direct laser writing Bessel beam technique, that is used in [18]. In that article, Liu & all have the ability to make channels with 300 nm diameters. They can also make a channel matrix with a 1.5 μm spatial period. Although this can be reduced to a few nanometers by choosing more precise mechanical parts for the experiment. Knowing this, we can say that it is therefore possible to reproduce the structure from [6] by using the Bessel beam laser technique (on a transparent material).

There are however limits to the resolution of this technique that become apparent if we look at another example shown in [6]. In this example (which has the same hole diameters and spatial period as the previous one), the authors increase the light trapping efficiency of the point defect by slightly changing the position of adjacent holes. This is shown in figure 1.3B. In this example, the adjacent holes are moved by approximately 60 nm to get the best efficiency of light trapping. The 60 nm resolution necessary here is not actually possible for laser techniques. This the limit of this laser technique (and the other ones too), it can make photonic crystals but it can not accurately tune their design.

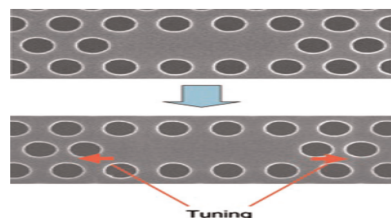


Figure 1.3B: Changing the position of adjacent holes to the point defect for better light trapping efficiency; source: [6]

II/ Nanofabrication techniques

In this part of the text, we shall look at the diverse techniques that are used for nanofabrication and optical metasurfaces manufacturing. These techniques are classified in 4 categories: direct write lithography, pattern transfer lithography, hybrid patterning lithography and Other potential techniques for metasurfaces fabrication. For each of these categories, we shall rapidly look at the specific techniques they comprise and give some of their specific features, such as resolution or speed. The intention is to compare these methods to the laser techniques, which are further explored in part III.

2.1/ Direct write lithography

2.1.1/ Electron beam lithography

Let's first look at direct write lithography techniques. The first one we shall look at is electron beam lithography (EBL). This technique is like traditional lithography, except for the fact that we use a focused Gaussian electron beam to expose the resist. This technique can produce very high quality photonic devices because of its extremely high resolution. In reference [7], where they use an aberration corrected electron beam to expose resist, and obtain feature sizes of around 2 nm. The resolution is excellent, however to do this, the researchers are using a scanning transmission electron microscope, which is a very complicated and expensive machine. This technique can not work at bigger scales, it is limited to the macroscopic scale. We note that it is also very slow. So, compared to EBL, the laser ablation techniques offer much lower resolution but they still enable the fabrication of optical metasurfaces on a macroscopic scale, with a much lowered complexity of use (no vacuum) and a more affordable price for manufacturing.

Figure 2.2 shows a schematic of how this technique works and Transmission electron microscope (TEM) images of obtained structures.

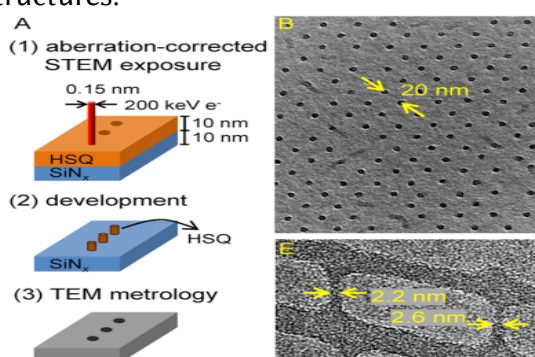


Figure 2.2: Schematic and results of EBL; image on the left show the working principle of the technique; TEM images on the right shows 2 nm feature size achieved with the technique; source: [7]

2.1.2/ Focused ion beam lithography

Focused ion beam lithography (FIBL) is a technique that uses a thin beam of ions to directly mill a material at the nanoscale. It can also be used to inscribe patterns in a resist layer, which can be

selectively etched later to form nanoscale structures. This ion beam is usually combined with an electron beam to allow for direct observation of the created structures. This technique combines an ion beam structure and a scanning electron microscope (SEM) structure to achieve ion beam resolutions under 10 nm and electron beam resolutions around 1 nm [8][9].

This method has many advantages. First, it's high precision. FIBL is only a bit less precise than electron beam lithography (<10 nm VS ~1 nm). Secondly the ion beam can be used to work on a sample that already has nanostructures, which is much less feasible with traditional mask lithography techniques [9]. A third advantage is the possibility to locally dope the sample with the particles of the ion beam. As an example, this can be used for making local hard masks that can be used for very precise selective etching (same resolution as stated previously).

This FIB approach also has many drawbacks. These are the long processing time for macroscopic structures, the high cost, the need to work under vacuum and the implantation of unwanted ions. Another drawback linked to the combination of FIB and SEM, is the need to coat the surface with a conductive layer to make it observable with an electron beam.

These problems make this technique not very useful for optical metasurfaces manufacturing. Indeed this method can only allow for prototyping of metasurfaces at a microscopic scale [4].

An example of the use of this technique for optical metasurfaces fabrication is presented in [10]. This paper presents a nanostructure that converts circularly polarized light into a focused optical vortex. This structure is tested for a laser beam of wavelength $\lambda=633$ nm.

This construction spans an area of 20 μm in diameter and is made of small elliptical cylinders.

These are 220 nm long along the long axis, and 66 nm long along the short axis. The cylinders are 180 nm thick. These structures are milled in 180 nm silver layer deposited on top of an SiO_2 substrate. The structure and its purpose are shown in figure 2.3

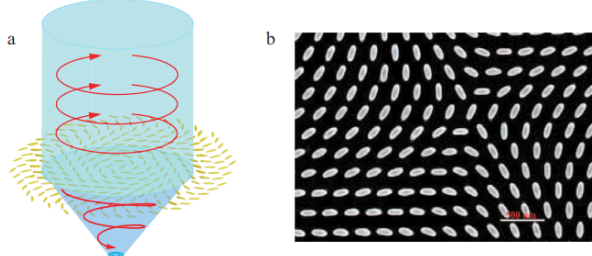


Figure 2.3: Metasurface for optical vortex generation and focus; on the left is a schematic of how the nanostructure converts circularly polarized light into an optical vortex; on the right is a SEM image of the structure, scale bar is represents 500 nm; the elliptical cylinders of the structure are 220 nm long along the long axis and 66 nm long along the short axis; source: [10]

2.1.3/ Laser lithography

Another method in the direct write lithography category, is laser interference lithography.

This technique uses two laser beams and makes them interfere to create a periodic interference pattern that can be used to expose a resist. This is used to create nanostructures spanning a large area and with great speed. This technique is very adapted for manufacturing metasurfaces on a large scale. It is used in [11] to create a periodic array of nanowires that are 200 nm high, 120 nm wide and separated from each other by a gap of 240. From [12], we can also see that the laser irradiation part is rapidly finished. Indeed, it takes 70s to irradiate an area of 2,5 mm radius.

This interference lithography approach has approximately the same resolution as the laser ablation techniques that are explored in III. This technique is also faster or as fast as the ablation methods, since the pattern is produced by interference and not by moving the laser beam.

However, this approach is much more complicated to implement since we have to use lithography and all the chemistry it involves. Figure 2.4 shows an image of the Au/Ag nanowires created in [11].

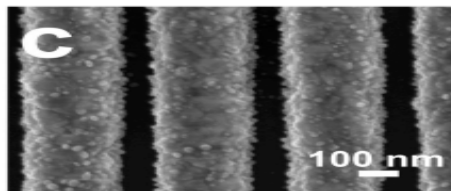


Figure 2.4: scanning electron microscope of Au/Ag nanowires; source: [11]

2.1.4/ Probe scanning lithography

This technique covers a silicone substrate with resist and a thin layer of silver (20 nm). It then uses an atomic force microscope (AFM) to scratch away the silver. This allows for pattern “scratching” tip and then selective etching. The authors make a negative index metasurface [13]. This technique allowed for a groove depth of 4 to 80 nm and a line width of 80 to 120 nm. The repeatability was 60 to 150 nm. This technique is good because it works under atmospheric condition and it has good precision. However, it is problematic because of its low width to depth ratio of lines, and because of its high price. Furthermore this technique is too slow and can not be used to make metasurfaces over large areas.

2.2/ Pattern transfer lithography techniques

2.2.1/ Plasmon lithography

This is a lithography technique that uses surface plasmon polaritons (SPPs) waves to expose a photoresist. The technique allows for subwavelenght resolution. An interface between a metal and a dielectric is used to generate the SPPs. This technique uses a mask with subwavelenght nanostructures. The SPPs use these nanostructures as concentration spots, which allow for a reproduction of these structures on the photoresist, even when the incident light has a much larger wavelength [4]. The photoresist can later be selectively etched, allowing for the production of nanostructures on the substrate of the photoresist.

As shown in [10], this technique can etch rectangles of 95 nm by 175 nm, with a period of 300 nm. This structure is used to make a hologram. The incident light, that comes onto the Cr mask used in this experiment, has wavelength of $\lambda=365$ nm and is linearly polarized.

The mask used is 9 μm by 9 μm , which shows one of the defaults of this technique. Macroscopic masks are difficult and expensive to produce[4]. Another problem is the complexity that comes with a lithography technique. Lithography is hard to implement and cannot be used for rapid prototyping, since the creation of an expensive mask is required. On the other hand the main advantages of this technique is that it is high throughput and low cost for mass production.

2.2.2/ Nano-imprint lithography

Nano-imprint lithography (NIL) is a technique that uses a reusable master mold to imprint a pattern into a moldable resist that can later be selectively etched. This resist can be shaped into the master bold by heat, by UV radiation or some other hybrid technique [4]. This nanofabrication method is good because it has a good resolution, it can pattern large surfaces (centimeter scale [14]), it can be setup for parallel fabrication, enabling mass production and finally, it is cheap. The problems with this technique are that it requires the fabrication of a precise master mold (which can be complex) and it required the used of plasma etching which can be complicated to implement. This is shown in [3], where the authors had to invent a new etching recipe for their heterogeneous nanoimprinted structure.

A first example of what can be achieved with this technique is shown in [14], where the authors made a master mold using interference laser lithography and used the mold for their NIL technique. They managed to make an aluminium nanowires grid on a glass substrate with a wire

thickness of 50 nm (showing the good resolution of the technique) and a height of 200 nm. This pattern spans and are of 5.5×5.5 cm 2 . The constructed device is a polarizer with an 85% transmission, working at a wavelength of 450 nm.

Figure 2.5 shows a transmission electron microscope (TEM) image of the structure and a schematic of NIL process.

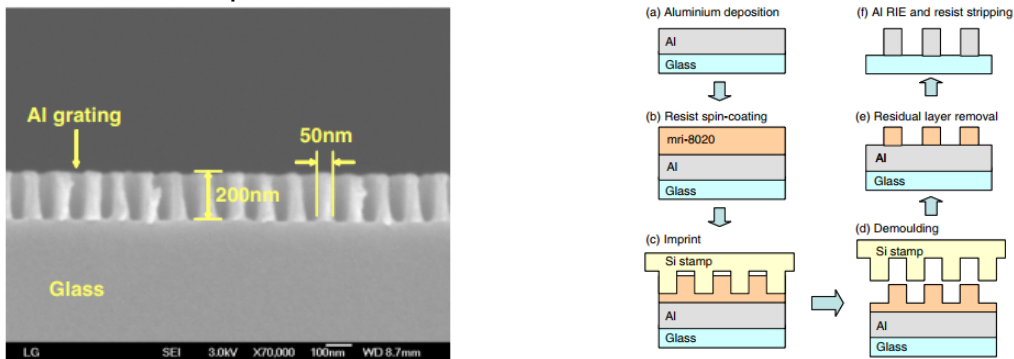


Figure 2.5: Structure microscope image and fabrication schematic; on the left is a TEM image of the aluminum grating showing the thickness and height of the nanowires; on the right a schematic if the NIL process showing the various steps, from molding to selective etching, by reactive ion etching (RIE); source: [14]

A second example of what the technique can do is shown in [3]. Here, the authors made an efficient broadband reflective metasurface by stacking multiple dielectric materials. This is harder to do than the first example, because it involves many materials. Here, following the previous example, they made a mold using the laser interference lithography technique, and used the mold to imprint a structure on a multilayered stack of materials. The structure is a grating of nanowalls made on an SiO₂ substrate. The walls are made of stacks of amorphous silicon (a-Si), under an SiO₂ layer, under an Si₃N₄ layer, under another a-Si layer. This is shown in figure 2.6. These walls are around 300 nm thick and 600 nm high [3]. The structure is a broadband reflector that above 90% of incoming light that has a wavelength between 600 nm and 800 nm. This structure is more complex than the first example because the multiple materials make the etching process more complex, since every material etched at a different rate.

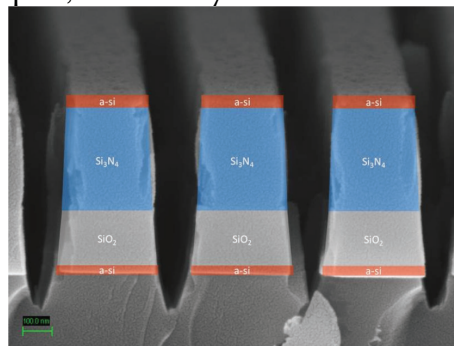


Figure 2.6: TEM image of a heterogeneous metasurface; this shows the metasurface nanostructure with the different materials; the scale bar is 100 nm; the walls are around 300 nm wide and 600 nm high; source: [3]

2.2.3/ Self-assembly lithography

These techniques use the self assembly of some nano-objects or a polymer to adjust a pattern that can be used for selective lithography etching. An example is the use of nanosphere lithography in [15] to make an Si cylinders metasurface that is used for sensing. The technique proceeds as follows: polystyrene (PS) nanospheres, with an average diameter of 350 nm, are deposited on a polyethylene terephthalate (PET) and Si substrate. The PET is 180 μ m thick. The

spheres and silicon are then etched by O₂ and we are left with Si cylinders. These are 330 nm in diameter and 170 nm high [15]. This technique is good for covering large surfaces at low cost and high speed but the patterns are not always uniform and their diversity is dictated by the number of patterns than can be self-assembled. We can not do any design we want.

Figure 2.7 shows a schematic of the fabrication process for this dielectric metasurface.

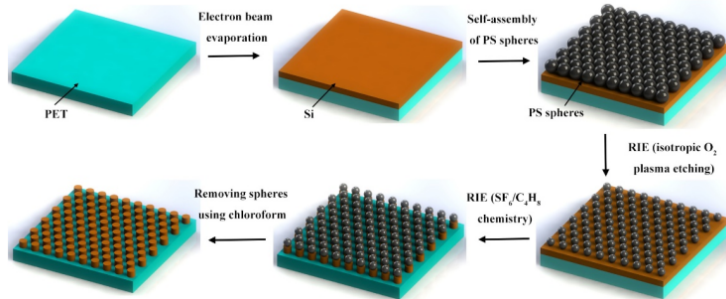


Figure 2.7: Schematic of fabrication using nanosphere lithography; source: [15]

2.3/ Other techniques for metasurfaces fabrication

2.3.1/ Laser induced forward lithography

This technique is called laser induced forward transfer or LIFT. This approach uses a femtosecond laser to blast away a local volume of metal or other material that is attached to a glass plate. The ablated material is shot through the glass and lands on a substrate's surface and forms the desired structures on it. Using paper [16], we note that this technique seem to be fit for working with features of around 1 μm. The spacing between two structures noted in [16] is 500 nm. This LIFT method has many advantages such as it's simplicity (and therefore low cost) and that it can produce any design that the laser can draw. However it seem to have less resolution than the laser ablation approach (500 nm vs 100 nm [17][16]) and article [16] reports a raster speed of 53,3 μm/s which is slower, compared to the 1 mm/s of ablation techniques.

Figure 2.1 shows a schematic of how this technique works.

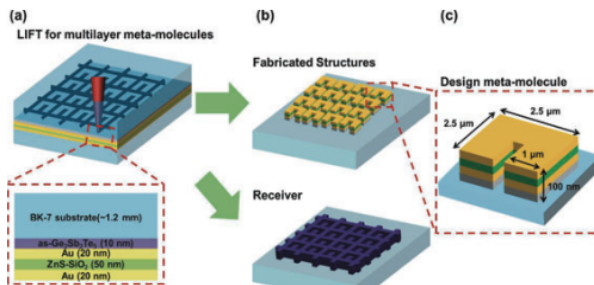


Figure 2.1: Schematic of how LIFT works; (a)A stack of material is blasted away by a laser, and (b) lands on a substrate, leaving the substrate with a nanostructure; source: [16]

2.3.2/ Laser ablation

We will now look at techniques that are not often used for optical metasurfaces fabrication but that offer new possibilities for the fabrication of metasurfaces. These methods usually uses a femtosecond or picosecond pulse to heat a very local volume of a material, which is then vaporized and leaves an empty channel behind. We will compare the other techniques to the femtosecond laser ablation technique. These laser methods can, at best, achieve channels with a diameter of around 100 nm and depths of around 7 μm [17][18]. This is achieved with a single pulse. The laser scanning speed is on the order of 1 or 2 mm/s.

III/ Laser techniques

In this part we shall explore multiple laser techniques and see what they can allow us to do. We will start by rapidly reviewing the physics at play between femtosecond laser pulses and the dielectrics they interact with. We will then look at techniques that play with the spatial and temporal form of the laser beam, in order to try to improve its ablation capabilities. We will also explore a technique that combines weak laser radiation and acid etching in order to be able to work with transparent crystals. At the end, we will compare the techniques in between themselves and talk about the advantages and drawbacks of each technique.

With ultrafast lasers it is possible to make diverse photonic structures, in diverse materials, provided that they are transparent to the laser light. Indeed, the nonlinearly-seeded ionization of the matter enables extremely accurate deposition of energy, at any location inside a transparent material. In order to compare the different techniques, we shall only look and compare simple structures such as single channels and channel matrices.

3.1/ Physics of ultrafast laser pulses interacting with dielectrics

When a femtosecond laser pulse hits a dielectric material (such as SiO₂, for example), it transfers its energy to the material through nonlinear ionization mechanisms [19]. This energy transfer happens because the pulse is powerful enough (10^{13} W/cm² and higher). These mechanisms allow for the generation of high temperature free electrons in the dielectric. Those electrons then transfer their energy to the material's lattice. This will produce various long term effects, depending on the pulse energy. If the pulse intensity is lower than the ablation threshold intensity, the pulse will result in effects such as refractive index changes (on the order of 10^{-3}) and material density changes.

If the pulse intensity is higher than ablation threshold intensity, then we get ablation (if the pulse is focused at the surface) or the creation of voids (if the pulse is focused inside the material).

The ionization mechanisms at play in these laser/matter interactions are shown in figure 3.1.

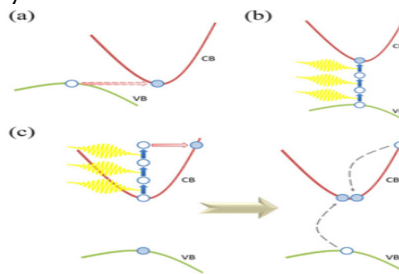


Figure 3.1: Ionization effects; (a)Tunneling ionization; (b)Multiphoton ionization; (c)Avalanche ionization; source: [19]

The nonlinear ionization effects are necessary for explaining photonic energy absorption in dielectrics because in those materials the electronic energy bandgap, between the valence band (VB) and the conduction band (CB), is too large (9 eV in fused silica). As a result visible light (from the sun, for example) can not excite electrons from the VB to the CB.

These nonlinear effects are tunnel ionization (figure 3.1.a), multiphoton ionization (3.1.b).

Avalanche ionization (3.1.c) is not a nonlinear ionization effect but it becomes important once free electrons start to accumulate in the CB as a result of the nonlinear effects. Tunnel ionization occurs when the electric field of the laser pulse is strong enough to distort the band structure of the dielectric. This allows the electrons to tunnel between the VB and the CB. Multiphoton ionization is the excitation of an electron to the CB via the simultaneous absorption of several photons. The total energy of the photons must be equal to or higher than the bandgap. In SiO₂, this effect requires the absorption of at least 6 photons [19]. Avalanche ionization happens when

an electron in the CB absorbs photons sequentially and acquires an energy (in reference to the bottom of the CB) that is higher than the bandgap energy. This electron can then use that energy to excite another electron from the VB to CB. This happens through collision between the two electrons.

Concerning these absorption effects, we note that they do not happen at the same timescale as other phenomenon such as melting and ablation. Indeed, these nonlinear effects happen at the femtosecond scale while melting happens at the picosecond scale (or more) and ablation happens at the nanosecond scale [20].

3.2/ Gaussian beams

A laser beam naturally presents a Gaussian profile. The simplest method to perform material processing is therefore to directly focus tightly such beam on small sizes. This is usually done by using high-numerical aperture microscope objectives as focusing elements. This Gaussian pulsed beam can be used to ablate transparent materials [17]. To use this technique, the beam is focused on (or under) the surface of the material. When a laser pulse is shot, the material gets ablated very locally with a depth of a few micrometers, depending on the energy used. When we want a deeper channel we can move the beam focus inside the material (by 1 μm for example [17]). We can keep doing that until we get the desired depth. A very important parameter for this technique to work is pulse duration. Here, the femtosecond laser pulse, must be stretched to 1 or more picoseconds. If we don't do this we can only get depths on the order of a few hundred nanometers. This is due to the intensity of femtosecond pulses which create a plasma at the surface, which absorbs/reflects the energy and prevents it from going deeper in the material [17] [18].

For this experiment to work one must prepare an appropriate optical stage (at the output of the laser) in order to modulate the pulse power and temporal shape. One also needs a precise, computer controlled, mechanical stage. The reachable spatial density of channels is directly function of this mechanical stage. The best positioning precision observed in the reference papers is ± 250 nm. It was observed in [21]. A useful mechanic stage for laser ablation of holes, for the making of metasurfaces and photonic crystals, should also be able to move at sufficient speeds. Speeds at least better than 1 mm/s should be achievable. Better mechanical stages than the ones observed in the references exist (1 nm resolution and sufficient speed). We can look for example at the V-551 precision linear stage from PI [22]. That device has a sensor resolution of 1 nm, a minimum incremental motion of 2 nm, a highest speed of 500 mm/s and a travel range going from 50 mm to 230 mm, depending on the model. These parameters are very suitable for the precise laser ablation of photonic devices. Finally, we remark that better channel depths are achieved if the focus is under the surface. 3 μm under the surface, for example.

This technique is used in reference [17] to ablate channels in SiO_2 . Channel diameters of 200-300 nm and channel depths of around 7 μm are obtained. This corresponds to an aspect ratio (depth/diameter) of around 30.

An example of a channel done with this technique is shown in figure 3.2. That image is extracted from [17]. It shows a channel with the above mentioned specifications.

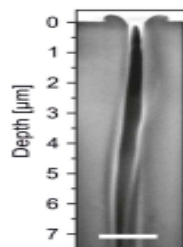


Figure 3.2: Channel ablated with Gaussian pulse; diameter: 200-300 nm; depth > 7 μm ; source: [17]

3.3/ Temporal shaping

The second technique we are going to talk about is similar to the previous one, except that the temporal shape of the beam has been changed. Here, a phase modulator is added to the optical stage in order to change the Gaussian temporal shape into an asymmetrical, picosecond long (>2 ps), series of low power femtosecond pulses with decreasing intensity. The pulses are followed by an even smaller and longer constant part. This picosecond pulse is shown in figure 3.3.

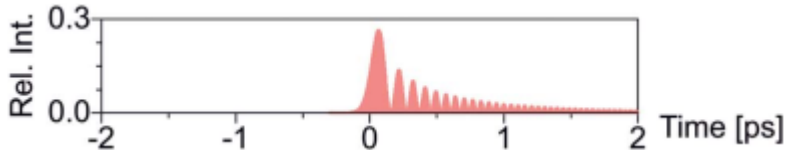


Figure 3.3: Pulse train; Relative intensity represented on Y axis and time represented on X axis;
source: [17]

These low energy femtosecond pulses (compared to the high energy single pulse used for ablation in the fs regime) are used because the energy they deposit is smaller than the ablation threshold energy, so they can go deeper into the material. We compare them to the even shorter and more powerful pulses used for femtosecond ablation, which get stopped at the surface of the material. Once the train of femtosecond pulses deposits their energy, the long constant part of the beam then comes along and gives the remaining necessary energy for ablation to happen. This technique allows us to slowly deposit energy without creating the surface plasma that gets rapidly created with femtosecond ablation, and reflects/absorbs the beam energy. This technique is more complex than the first one but it allows to correct some limitations. Indeed, with this technique, we get more straight and homogeneous channels [17]. That crooked channel problem of the first technique can be observed in figure 3.2.

This technique, like the other one, allows us to get holes with a diameter of 200-300 nm. We get pore depth of around 7 μm too. These test channels have been ablated in SiO_2 .
Also like the other technique, we get better depths if we aim the focal point under the surface of the material.

3.4/ Spatial beam shaping

Here, instead of playing with the temporal form of the beam, we modify its spatial form. In order to realize this we make the laser Gaussian beam go through a conical lens, also called axicon. At the output of that lens we get a Bessel beam [18][23]. This beam doesn't ideally diffract and is much more robust (gets less deformed) than the Gaussian beam, when used for material ablation. The Bessel beam allows for the ablation of straight and homogeneous channels. As implemented in [18], this method also uses an annular aperture after (or before) the axicon. This helps with the reduction of the depth of field (DOF) to 20 μm . Like with the other techniques, here, a microscope lens is also used to focus and reduce the beam to a diameter (full width half maximum) of around 970 nm, in air. The smallest channel diameter achieved with this technique in [18] is approximately 300 nm. The hole depth corresponding to that diameter is around 1 μm . This was done in an SiO_2 sample. Deeper channels can be obtained by increasing the pulse energy. Hole depths up to 28 μm can be obtained. We remark however that increasing the energy, will also increase the channel diameter. And this will also give us a less clean hole entry (rings of matter appear around the channel entrance). For this technique, it is recommended (by [18]) to stretch the femtosecond pulse into a 1 picosecond one. This gives better channel depths. Indeed, pulses that are in the femtosecond regime can only make channel depth in the order of 100 nm. If deeper holes are wanted, then picosecond long pulses should be used [17][18].

Figure 3.4, show a schematic of the experiment, and a graph showing the experimentally measured evolution of channel diameter and channel depth as a function of pulse energy. This pulse length used is 1 ps.

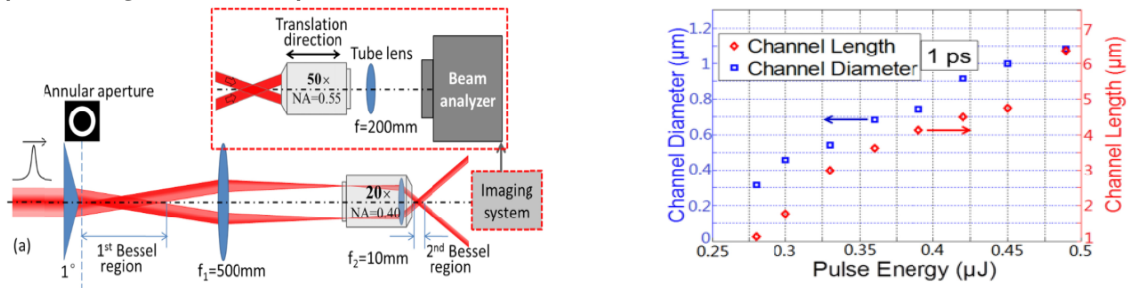


Figure 3.4: Schematic and pore parameters as a function of energy; The schematic on the left show the optical system used to generate and focus the Bessel beam; The graph on the right, shows channel diameter and depth as function of pulse energy (pulse length of 1 ps); source: [18]

3.5/ Combination of laser irradiation and chemical etching

Another technique that is used in reference [21], and that uses a femtosecond laser, is a technique that combines the laser beam with an acid etching process.

This hybrid procedure has been developed for the etching of holes in crystalline and transparent materials such as yttrium aluminium garnet (YAG) or sapphire. This technique is used to avoid cracks that sometimes happen in crystals when one tries to nanostructure them with an ultrafast laser pulse. For the implementation of this method, a focused Gaussian beam is used for material irradiation. A femtosecond pulse is used (350 fs pulses are used in [21]). The pulse Energy is under the ablation threshold. We do this because we wan to use the laser to change the chemical reactivity of the material. This will help because it makes the acid etching speed much greater, in the volume containing those chemical changes. Etching speed is greatly improved by a factor of around 10^5 . This results in the etching selectivity of the irradiated volumes being greatly improved. For example an irradiated volume, in YAG, goes from an etching speed of 0,6 nm/h to a much greater speed of 100 μm/h. The etching rate is multiplied by 1.6×10^5 [21]. The selectivity of this etching process is excellent. After exposing a very localized volume to the laser beam and in the material, we can then polish the sample to expose the irradiated material. The next step after that is to select an appropriate acidic solution, which will change depending on the material we work with. From the information given by [21], an acidic solution containing 44% by weight phosphoric acid and deionized water, should be used to etch YAG. The solution is also heated at 350 K (76,85 °C) and mixed during the whole etching process. For sapphire, a solution of 20% by weight Hydrofluoric acid and deionized water is required. This solution must also be heated to 308 K (34.85 °C) in an ultrasonic bath, during the entire etching process. The etching step may last a long time. To illustrate this, we can look at reference [21] which gives us the following example: to engrave pores in YAG, with openings of $368 \times 726 \text{ nm}^2$ and depths of 3.1 mm, one must wait 170h for the acid etching process to end.

The next and final step done in this technique, is cleaning. The sample must be taken away from the etching solution and sequentially washed in a deionized water ultrasonic bath, then in an acetone ultrasonic bath and finally in an ultrasonic methanol bath.

From reference [21], we see that it is possible to make channels with a diameter of around 110 nm in YAG and pores of around 121 nm in sapphire. These are the best channel diameters obtained in that paper. To the author's knowledge these diameters are also the best obtained results for this technique. The range of obtainable depth is quite large, it can go from a few micrometers to a few millimeters (or more if we are willing to wait the etching time). These channels are slightly asymmetrical in terms of diameter. Indeed, in the examples given by [21], the width over height aspect ratios vary from 1.20 to 1.45.

For this technique, one can change the diameter of a channel by changing the laser pulse energy. This can be used to vary a hole's diameter along the depth. If a hole is irradiated by multiple laser pulses, we can change the pulse energy at each shot, this will result in a changing channel diameter along the depth.

This is harder to do with the other techniques because when laser pulse energy is changed, it also modifies the depth of channel. Here, a Gaussian pulse is used and the material removal is done by the acid, so the laser energy has less consequences on the pore depth. It has more to do with focal point positioning.

This technique (always as implemented in [21]) allows for a wall thickness between two channel, of around 250 nm. The technique also allows for a highest fill factor (FF = volume of hole/volume of material) of 44%. Having the capacity to play with this parameter is important for photonic structure manufacturing. Figure 3.5, shows a SEM image of a channel matrix in YAG, with an FF of 44%. In this example the channels are asymmetrical with a front area of $276 \times 972 \text{ nm}^2$. The reason for this is not explained in [21]. We can suppose that it may be due to overlapping laser pulses or uncontrolled laser light propagation. And because of the size of these channels, the wall thickness is reduced to 150 nm. By playing with the FF, it is possible to change the wall thickness. Each of these channels has a depth of 1 mm.

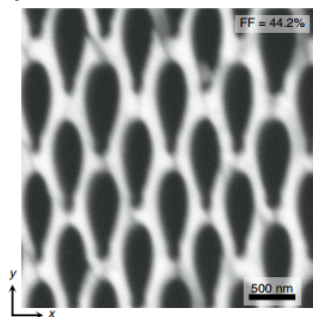


Figure 3.5: Channel matrix; FF = 44.2%; Etched in YAG; Channel front area= $276 \times 972 \text{ nm}^2$; Wall thickness between 2 channels = 150 nm; Channel depth = 1 mm; source: [21]

3.6/ Discussion: comparison of experimental techniques

Now, let us compare these previous four techniques. We will first start by listing the things they have in common. First, the advantage with these femtosecond (or picosecond) laser techniques is that they allow us to structure materials at the 100 nm scale (or bigger), without the need for traditional lithography techniques. Direct laser writing removes the need for expensive lithography masks. Indeed, the biggest advantage of these laser techniques is the ability to modify a design with much more ease, speed and lower cost. Here, there is no need to manufacture a new expensive mask with complicated techniques such as Focused Ion Beam (FIB), every time we need to change the design.

A second common point between these methods is the use of an optical stage and a mechanical stage. The optical stage is used to modify the beam shape (temporally and spatially) and modulate pulse energy. The mechanical stage controls the precise positioning of the laser and therefore the channels spatial density. It also controls the speed at which the pores get ablated. The mechanical stage must be chosen as having the highest possible accuracy (1 nm would be very good), while keeping a good speed ($>1 \text{ mm/s}$). With high precision and speed, high quality photonic crystals (2D metasurfaces) can be made.

A third point, these techniques have in common, is the laser pulse duration. For each one, of the techniques it is better to use a beam of a few picoseconds length. It is also better if the focal point of the beam is positioned under the surface ($3 \mu\text{m}$ deep, for example). This positioning of the focal point allows for higher channel depths. A last common point worth mentioning is that, for these techniques are in transparent media (or transparent for the relevant wavelengths). Indeed, if we

want to make 3D nanostructures for metasurfaces or photonic crystal manufacturing, we need to work with a material where light can easily propagate.

Now that we have talked about the common points, we can start looking at each technique individually and discuss its advantages and drawbacks.

Let's start with the first technique, which uses a simple Gaussian beam (temporal and spatial) to ablate. Compared to the other techniques, this one has the advantage of being the simplest one to implement. It has, however many defaults. One of those, is the plasma that gets created at the surface of the material and absorbs/reflects pulse energy. This plasma appears when the femtosecond pulses are used. When this happens pulses are only able to produce channel depths on the order of 100 nm. To produce channel depths on the order of 1 μm with this technique, one must stretch that femtosecond pulse into a picosecond one. Another drawback is that the Gaussian beam used in this technique is non robust and prone to deformation, when used for ablation. This produces distorted channels, as can be seen on figure 3.2.

There is also an energy efficiency drawback. As shown in [17], this single Gaussian pulse, is not very efficient at transferring energy to the lattice.

The hole diameters made with this technique range from 200 to 300 nm, which is acceptable but is not as good as the 100 nm diameter obtained by the laser-acid technique.

For the second method, which changes the temporal shape of the pulse into a train of femtosecond pulses, we can start by talking about the main disadvantage. This main drawback is an augmentation of the complexity of the optical stage. This complexity arises because of the need to add a phase modulator into the optical path of the beam. This phase modulator is what temporally shapes the beam for this technique.

A first advantage of this technique is that it can overcome the plasma surface absorption problem, that appears in the first method (if the Gaussian pulse is not temporally elongated) we looked at. This improvement allows us to make deeper and straighter holes ($>7 \mu\text{m}$, compared to a few hundred nanometers). Indeed, this also solves the crooked channel fabrication problem we used to have with the simple (temporally elongated) Gaussian beam method. A second advantage, is that this method is more efficient than the others at depositing energy that contributes to the ablation.

Channel diameters made with this technique are a little smaller than those obtained with the focused Gaussian beam technique, but they are still in the same area of 200 to 300 nm. They are also in the same range as the diameters obtained with the Bessel beam procedure technique which allow for 230 nm channel diameters, at best [24].

Let's now look at the advantages offered by the Bessel beam technique. The first advantage of the technique is, as for the second method, that it can solve the surface plasma absorption problem, that appear for Gaussian femtosecond pulses. By changing the spatial form of the beam (as opposed to the temporal shape, for the second method), it becomes possible to make very straight channels, whose depths can range from 3 μm to 28 μm . We remark however, that the deeper channels (28 μm for example), require more energy to ablate, and that also leads to the appearance of matter rings around the entrance of the channel. These non-clean channel entrances force to add a polishing step into this technique's protocol, if we want clean channel entrance.

Channel diameters (230 nm), as stated previously, are around the same size as the ones obtained with the other techniques. A second benefit of the truncated Bessel technique used in [18], is its lower depth of field (DOF), which allows it to obtain a less elongated Bessel beam and which permits for better energy focusing. This second benefit, is obtained by placing an annular aperture before or after the conical lens. An easily noticeable problem with this aperture, however, is that it makes us lose up to 86% of beam energy (since a significant part of the beam is blocked by the

aperture). This is not a problem in this case, since the laser setup can provide enough energy to overcome this loss. But it is still a drawback for systems that might be limited in terms of energy.

The last method we shall discuss, is the one combining weakening of the material by laser and acid etching. This method is very interesting since it allows for the fabrication of the smallest hole diameters (around 100 nm) among the other laser techniques, while allowing for millimeter deep holes. The hole matrices made with this technique have the highest fill factor (44%), compared to the other laser techniques. A notable advantage of this technique is that it works on transparent crystals at macroscopic scales and without propagating cracks in the crystal, which is different for the other techniques, that may sometimes create these cracks. Another advantage of this procedure, that must be noted, is that it allows us to vary the channel diameter as a function of depth. This is harder to do with the other approaches because their pulses use more energy, which will ablate volumes that are deeper than the penetration depth allowed by a weaker pulse (as the one used in the laser-acid technique). This results in the fact that we have more channel depth control with this technique. For example, with the laser-acid approach we would be able to change diameters along depth, with 1 μm steps (1 μm is the depth axis resolution in [21]), while with the other methods, we would only be able to have >7 μm steps. This approach also allows us more ease when doing more complex channel geometries, since we do not have to worry about matter getting stuck somewhere, as might happen with the other laser ablation methods. Indeed, this does not happen with acid etching.

Despite all its advantages, this approach also has a few drawbacks. The first one that we notice, is about the complexity. Indeed, with this method, we have a chemical step that must be taken into account. This step must be optimized each time we deal with a different material. We must also notice the need to implement safety protocols when working with acids. A second problem is the difficulty of working with birefringent materials. These duplicate the light beam, which results in 2 holes appearing after etching, instead of 1.

One last problem, that appears with this laser-acid approach, is the etching time which may take many days, depending on hole size. For example, a millimeters deep channels takes 170h etching time in YAG [21]. This may be problematic if this technique is used for quick prototyping of metasurfaces which one might want to rapidly change and create. But if we just need to produce many of the same sample, then we can just put all the samples in the same acid bath, after the radiation step. They will all be etched in the same amount of time, making the production time acceptable.

The following tables will summarize the advantages and drawbacks of each technique seen in the references of this text.

Gaussian beam with adapted pulse duration

Advantages	Drawbacks
Simplicity	Non uniform propagation of beam in material
Intermediate channel diameter	Distorted channels
	Low energy transfer efficiency

Temporally-shaped pulse

Advantages	Drawbacks
Straight and homogeneous channels	Complexity
Good optical energy transfer to material	
Intermediate channel depth and diameter	

Truncated Bessel beam technique

Advantages	Drawbacks
Robust beam	Large channel diameter (compared to the other 3 techniques)
Deep channels	Unclean hole entrance if too much energy is used
Straight channels	May require polishing
Single energy maxima along the beam	

Laser-acid technique

Advantages	Drawbacks
Better compatibility with crystals	May not work with birefringent materials
Best channel diameters	More complex than other techniques
Best channel depths	Long etching time
Low energy laser irradiation allows for higher freedom in channel design	
Best fill factor	
Lowest wall thickness between 2 pores	

These techniques could be enhanced by experimenting with diverse improvement strategies. We could, for example, change the wavelength used (IR or visible) and go down to the UV. This might give us better resolutions. This is similar to what is done in lithography when one wants better resolutions.

3.7/ Overview

With the help of laser techniques, it is possible to make channels in transparent media, with a minimal diameter of around 100 nm in crystals [21] and 230 nm in amorphous materials [24]. The depth of these holes can vary between a few micrometer and a few millimeters (and more if needed) [21][23][18]. Regarding spatial density of the channels, it is possible to have 133 nm [21] or 600 nm[24] of spacing in between two channels, depending on the technique used. Hole diameter accuracy also varies with technique used. At best, we get variations on the order 10 nm [21]. We also get variation on the order of 100 nm, with less accurate techniques [25]. In order to have a better representation of the channels we are dealing with here, we show an example of a channel matrix in figure 3.6 [21]. This Scanning electron microscope (SEM) image shows channels arranged in a hexagonal pattern. The holes have a mean diameter in the X direction of 109 nm and 125 nm in the Y direction. There is a mean wall thickness (separation between two holes) of 250 nm. The filling factor (FF), which is channels volume/material volume, is 18.2%.

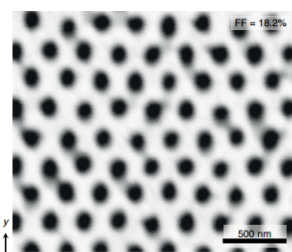


Figure 3.6: Hexagonal matrix of channels; Wall thickness = 250nm; Diameter X = 109 nm & diameter Y = 125 nm; source: [21]

We note that with the technique used to make this matrix, it is possible to raise the FF up to 44%. We also note that it is possible to diminish the wall thickness to 150 nm if we play with this FF parameter (remembering, of course, that this will make the channel diameter wider). Depending on the technique used, it is also possible to change the channel diameter as function of depth. We can also make channels oriented at an angle with the surface [21].

IV/ Analysis techniques of laser nanofabricated structures

In this part, we will rapidly look at the different techniques that are used to analyze the structures made with the laser techniques. We will talk about the main techniques that are used in the literature. These techniques are Scanning electron microscopy, atomic force microscopy and light microscopy.

4.1/ Scanning electron microscopy

One of the most used techniques for the analysis of the structures made with the different laser techniques is scanning electron microscopy (SEM). This is a well known technique, where a focused beam of electron is shot at a sample and interacts with the atoms. This results in many signals, but usually secondary electrons are the one that are used for imaging. The number of measured secondary electrons gives the intensity at a given spot. By scanning the electron beam across the sample, an image of the surface is produced. This technique has a resolution of around 1 nm. However this can change a little depending on the machine used. For example, the scanning electron microscope from the Helios NanoLab 650 machine [8] has a sub 1 nm resolution, but the Phenom Pro Desktop machine has a resolution of 6 nm [26].

This technique works in a vacuum chamber and also requires the sample surface to be conductive. Usually a non-conducting sample is coated with a thin layer of metal to prevent the unwanted accumulation of charges. To analyze the channels made by the laser techniques, the FIB technique is used to mill the holes and cut them in half. This allows us to look at the insides of channels with the SEM. This way, we can see if a channel keeps its radius along the depth, and we can see if the hole still contains non ablated material. Figure 4.1 shows images obtained with this SEM technique. Image on the left is coming from [17] and shows a 200-350 nm hole made with a temporally shaped femtosecond pulse. Image on the right comes from [25] and shows 230 nm holes made with a femtosecond Bessel beam pulse.

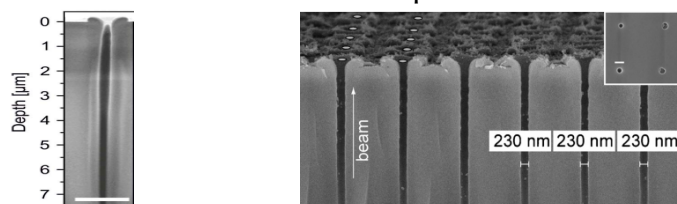


Figure 4.1: SEM images; on the left 200-350 nm hole; on the right is 230 nm series of holes;
sources: [17] for image on the left and [24] for image on the right

This technique can also be combined with polishing. As shown in [25], polishing can be used to expose channel length from the side. It can be used on a matrix of identical holes in order to cut one of them in half, so that it can be observed. It can also be used to expose the channels from the front, by removing matter layer by layer. This is done in [25] with an average material removal step of 6.7 μm .

4.2/ Atomic force microscopy

Atomic force microscopy is also a well known technique where a nanometer scale tip is used to sense inter-molecular forces between the tip and the surface it sensing. As shown in [27], this

technique has a resolution in the order of 10 nm (for the microscopes that are used in air). This number can be a little higher or a little lower depending on the machine used. We note that atomic force microscopes have a better resolution in the vertical axis than in the XY axis. This technique is used in [25] to measure the opening of a channel.

Figure 4.2 shows an image obtained by AFM of channel openings, with a bar indicating height.

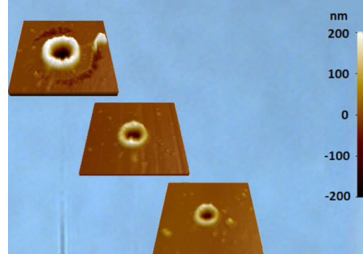


Figure 4.2: AFM measurements; this shows three AFM measurement of channels drilled with femtosecond Bessel beams with decreasing energy (starting from the top one); the bar on the right indicates height; source; [25]

4.3/ Light microscopy

This technique uses a conventional light microscopes to look at microstructures. At best this technique has a resolution of 200 nm [32]. This technique is useful for looking at transparent materials. A transmission microscope or a reflection microscope can be used. It is also possible to use confocal microscopy to recreate 3D images of the structures. Light microscopy is useful because it is very easy to use and works very well if the structures are large enough (around 1 μm or bigger). However if the structures are too small, this technique not longer useful. This problem is very notable since, the structures we look at in this text, are often on the order of 100 nm

Conclusion

In this text we have looked at dielectric metasurfaces and photonic crystals and their feature sizes. We have looked at nanofabrication techniques and then focused on direct laser writing techniques. We looked at the advantages and drawback of these laser techniques and found that the most promising (in terms of resolution) technique was the one that combined the femtosecond laser pulse with an etching acid solution. We also rapidly looked at the common analysis techniques used for inspecting nanostructures. Finally, when we looked at the feature sizes of the photonic structures made with metasurfaces and photonic crystals, we found that it was possible to make them with the direct writing laser techniques. We found however that is not possible to precisely tune the design of these structures because of the lack of resolution of these methods.

References:

- [1] Metasurfaces: subwavelength nanostructure arrays for ultrathin flat optics and photonics, Rho, J. (2020). *MRS Bulletin*, 45(3), 180–187. 2020
- [2] All-Glass, large metalens at visible wavelength using deep-ultraviolet projection lithography, Joon-Suh Park, Joon-Suh Park, Shuyan Zhang, Alan She, Wei Ting Chen, Peng Lin, Kerolos M. A. Yousef, Ji-Xin Cheng, and Federico Capasso, *Nano Lett.* 2019, 19, 12, 8673–8682
- [3] All-dielectric heterogeneous metasurfaces as an efficient ultra-broadband reflector, Yuhan Yao, Wei Wu, *Adv.OpticalMater.*2017, 5, 1 700 090
- [4] Advances in optical metasurfaces: fabrication and applications, Vin-Cent Su, Cheng Hung Chu, Greg Sun, and Din Ping Tsai, *Optics Express* Vol. 26, Issue 10, pp. 13 148-13 182 (2018)
- [5] Recent advances in planar optics: from plasmonic to dielectric metasurfaces, Patrice Genevet, Federico Capasso, Francesco Aieta, Mohammadreza Khorasaninejad, and Robert Devlin, *Optica* Vol. 4, Issue 1, pp. 139-152 (2017)
- [6] Photonic crystals, S. Noda, FT Mahi, H Zappe, *Comprehensive Microsystems*, 2008, Pages 101-112
- [7] Resolution limits of electron-beam lithography toward the atomic scale, Vitor R. Manfrinato, Lihua Zhang, Dong Su, Huigao Duan, Richard G. Hobbs, Eric A. Stach and Karl K. Berggren , *Nano Lett.* 2013, 13, 4, 1555–1558
- [8] <http://www.nanocenter.si/uploads/PDF/NAVODILA%20ZA%20OPREMO/Helios-NanoLab-650-ds-web.pdf> (this is a technical documentation of a FIB-SEM instrument)
- [9] Wanzenboeck, Heinz & Waid, Simon. (2011). Focused Ion Beam Lithography (updated in 2014) (chapter 2 of the book)
- [10] A planar chiral meta-surface for optical vortex generation and focusing, Xiaoliang Ma, Mingbo Pu, Xiong Li, Cheng Huang, Yanqin Wang, Wenbo Pan, Bo Zhao, Jianhua Cui, Changtao Wang, ZeYu Zhao & Xiangang Luo, *Sci Rep* 5, 10 365 (2015)
- [11] Large-Scale Fabrication of Porous Gold Nanowires via Laser Interference Lithography and Dealloying of Gold–Silver Nano-Alloys, Adrien Chauvin, Nicolas Stephan, Ke Du, Junjun Ding, Ishan Wathuthanthri, Chang-Hwan Choi, Pierre-Yves Tessier and Abdel-Aziz El Mel, *Micromachines* 2017, 8(6), 168
- [12] Using laser interference lithography in the fabrication of a simplified micro and nanofluidic device for label free detection, Taiga AJIRI, Haruya KASA, Masatoshi MAEKI, Akihiko ISHIDA, Hirofumi TANI, Junji NISHII, Manabu TOKESHI, 2017 Analytical sciences Volume 33 Issue 10 Pages 1197-1199
- [13] Nanofabrication of negative refractive index metasurfaces, Zoran Jakšić Dana Vasiljević-Radović Milan Maksimović Milija Sarajlić Aleksandar Vujanić Zoran Djurić, *Micoelectronic Engineering* Volume 83, Issues 4–9, April–September 2006, Pages 1786-1791

- [14] Fabrication of a 50 nm half-pitch wire grid polarizer using nanoimprint lithography, Seh-Won Ahn, Ki-Dong Lee, Jin-Sung Kim, Sang Hoon Kim, Joo-Do Park, Sarng-Hoon Lee and Phil-Won Yoon, *Nanotechnology* 16 1874, 2005
- [15] Flexible, all-dielectric metasurface fabricated via nanosphere lithography and its applications in sensing, Guanqiao Zhang, Chuwen Lan, Hui long Bian, Rui Gao, and Ji Zhou, *Optics Express* Vol. 25, Issue 18, pp. 22038-22045 (2017)
- [16] Fabrication of multilayer metamaterials by femtosecond laser-induced forward-transfer technique, M.L. Tseng, P.C. Wu, S. Sun, C.M. Chang, W.T. Chen, C.H. Chu, P.L. Chen, L. Zhou, D.W. Huang, T.J. Yen, D.P. Tsai, *Laser Photonics Rev.* 6, No. 5, 702–707 (2012)
- [17] Temporal airy pulses for controlled high aspect ratio nanomachining, Nadine Götte, Thomas Winkler, Tamara Meini, Thomas Kusserow, Bastian Zielinski, Cristian Sarpe, Arne Senftleben, Hartmut Hillmer, and Thomas Baumert, *Optica* Vol. 3, Issue 4, pp. 389-395 (2016)
- [18] Truncated gaussian-bessel beams for short pulse processing of small-aspect-ratio microchannels in dielectrics, Xing Liu, Qingfeng Li, Aurélien Sikora, Marc Sentis, O. Uteza Razvan Stoian, W Zhao, G Cheng, N. Sanner, *Optics Express*, Optical Society of America, 2019, 27 (5), pp.6996. 10
- [19] Investigation of ultrafast laser photonic material interactions: challenges for directly written glass photonics, M. Ams, G.D. Marshall, P. Dekker, M. Dubov, V.K. Mezentsev, I. Bennion, M.J. Withford, *IEEE Journal of Selected Topics in Quantum Electronics* (Volume: 14, Issue: 5, Sept.-oct. 2008), 1370 - 1381
- [20] Modelling ultrafast laser ablation, Baerbel Rethfeld, Dmitriy S Ivanov, Martin Garcia and Sergei I Anisimov, *J. Phys. D: Appl. Phys.* **50** (2017) 193001
- [21] Three-dimensional femtosecond laser nanolithography of crystals, AiránRódenas, Min Gu, Giacomo Corrielli, Petra Paiè, Sajeet John, Ajoy K. Kar, Roberto Osellame, *Nature Photonics* volume 13, pages 105–109(2019)
- [22] <https://www.physikinstrumente.com/en/products/linear-stages/stages-with-pimag-magnetic-direct-drive-linear-motor/v-551-precision-linear-stage-1200204/>
- [24] High aspect ratio nanochannel machining using single shot femtosecond Bessel beams, M. K. Bhuyan, F. Courvoisier, P. A. Lacourt, M. Jacquot, R. Salut, L. Furfarò, and J. M. Dudley,
- [25] Front-surface fabrication of moderate aspect ratio micro-channels in fused silica by single picosecond Gaussian-Bessel laser pulse, Xin Liu, Nicolas Sanner, Marc Sentis, Razvan Stoian, Wei Zhao, Guanghua Cheng, Olivier Utéza, *Applied Physics A* **volume 124**, Article number: 206 (2018) *Applied physics letters* 97, 081102, 2010
- [26] <https://www.thermofisher.com/fr/fr/home/electron-microscopy/products/desktop-scanning-electron-microscopes/phenom-pro.html#specifications> (specifications for the Phenom Pro Desktop SEM)
- [27] <https://www.afmworkshop.com/afm-products/atomic-force-microscopes/tt-2-afm> (The TT-2 AFM specifications)

[28] <https://www.aerotech.com/product-catalog/stages/linear-x-y-stages/ant95xy.aspx?p=%2fproduct-catalog%2fstages%2flinear-x-y-stages.aspx>

[29] Investigation of ultrafast laser-photonic material interactions: challenges for directly written glass photonics, M. Ams, G.D. Marshall, P. Dekker, M. Dubov, V.K. Mezentsev, I. Bennion, M.J. Withford, IEEE Journal of Selected Topics in Quantum Electronics (Volume: 14, Issue: 5, Sept.-oct. 2008)

[30] Batch fabrication of metasurface holograms enabled by plasmonic cavity lithography, Liqin Liu, Xiaohu Zhang, Zeyu Zhao, Mingbo Pu, Ping Gao, Yunfei Luo, Jinjin Jin, Changtao Wang, and Xiangang Luo, Adv.OpticalMater.2017, 5, 1700429

[31] Direct laser-written integrated photonics devices including diffractive optical elements, Jiyeon Choi, Mark Ramme, Martin Richardson, Optics and Lasers in Engineering Volume 83, August 2016, Pages 66-70

[32] <https://www.microscopyu.com/microscopy-basics/resolution>